AIP | Review of Scientific Instruments

A high pressure x-ray photoelectron spectroscopy experimental method for characterization of solid-liquid interfaces demonstrated with a Li-ion battery system

Julia Maibach, Chao Xu, Susanna K. Eriksson, John Åhlund, Torbjörn Gustafsson, Hans Siegbahn, Håkan Rensmo, Kristina Edström, and Maria Hahlin

Citation: Review of Scientific Instruments **86**, 044101 (2015); doi: 10.1063/1.4916209
View online: http://dx.doi.org/10.1063/1.4916209
View Table of Contents: http://scitation.aip.org/content/aip/journal/rsi/86/4?ver=pdfcov
Published by the AIP Publishing

REVIEW OF SCIENTIFIC INSTRUMENTS **86**, 044101 (2015)

A high pressure x-ray photoelectron spectroscopy experimental method for characterization of solid-liquid interfaces demonstrated with a Li-ion battery system

Julia Maibach,[1] Chao Xu,[1] Susanna K. Eriksson,[2] John Åhlund,[3] Torbjörn Gustafsson,[1] Hans Siegbahn,[4] Håkan Rensmo,[4] Kristina Edström,[1] and Maria Hahlin[4,a)]

[1]*Department of Chemistry–Ångström Laboratory, Uppsala University, Box 538, SE-751 21 Uppsala, Sweden*
[2]*Department of Chemistry–Ångström Laboratory, Uppsala University, Box 523, SE-751 20 Uppsala, Sweden*
[3]*VG Scienta AB, Box 15120, SE-750 15 Uppsala, Sweden*
[4]*Department of Physics and Astronomy, Uppsala University, Box 516, SE-751 20 Uppsala, Sweden*

(Received 8 October 2014; accepted 12 March 2015; published online 6 April 2015)

We report a methodology for a direct investigation of the solid/liquid interface using high pressure x-ray photoelectron spectroscopy (HPXPS). The technique was demonstrated with an electrochemical system represented by a Li-ion battery using a silicon electrode and a liquid electrolyte of $LiClO_4$ in propylene carbonate (PC) cycled versus metallic lithium. For the first time the presence of a liquid electrolyte was realized using a transfer procedure where the sample was introduced into a 2 mbar N_2 environment in the analysis chamber without an intermediate ultrahigh vacuum (UHV) step in the load lock. The procedure was characterized in detail concerning lateral drop gradients as well as stability of measurement conditions over time. The X-ray photoelectron spectroscopy (XPS) measurements demonstrate that the solid substrate and the liquid electrolyte can be observed simultaneously. The results show that the solid electrolyte interphase (SEI) composition for the wet electrode is stable within the probing time and generally agrees well with traditional UHV studies. Since the methodology can easily be adjusted to various high pressure photoelectron spectroscopy systems, extending the approach towards operando solid/liquid interface studies using liquid electrolytes seems now feasible. [http://dx.doi.org/10.1063/1.4916209]

INTRODUCTION

In electrochemical systems, the conversion between electrical and chemical energy occurs through redox reactions in the interface region between a solid electrode material and most often a liquid electrolyte. Improvements of such systems when it comes to efficiency, long term stability, etc., require in-depth knowledge of the composition, formation, and chemical processes occurring at these interfaces under operating conditions.[1] For example, in Li-ion batteries the first lithiation process is accompanied with an irreversible loss of cycleable lithium due to the formation of an interphase layer at the negative electrode. This functional layer is referred to as the solid electrolyte interphase (SEI),[2–4] and the composition of the SEI largely influences the short and long-term performance of the battery. Therefore, understanding the formation, composition, and dynamics of the SEI is a key question in Li-ion battery development.

A variety of characterization techniques have been applied to investigate SEI formation, such as atomic force microscopy (AFM), scanning electron microscopy (SEM), transmission electron microscopy (TEM), X-ray photoelectron spectroscopy (XPS), and Fourier transform infrared spectroscopy (FTIR).[3,5] Among all these techniques, XPS, with its high surface sensitivity, is a technique perfectly suited to study the composition of the interfaces in Li-ion batteries and has as such already been widely used in this field.[6–11] Specifically, the combination of synchrotron radiation based soft and hard x-ray photoelectron spectroscopy is capable of yielding comprehensive information about the SEI through non-destructive depth-profiling.[6,10,12–14]

Traditionally, electron spectroscopy has been limited to measurements under high to ultrahigh vacuum conditions (UHV) (below 10^{-6} mbar). The recent instrumental developments, e.g., introducing efficient differential pumping systems, have relaxed the vacuum constraints, and the field of high pressure x-ray photoelectron spectroscopy (HPXPS) has developed.[15] The growth of new instrumentation for HPXPS systems has been very rapid during the past years both when it comes to in-house and synchrotron based setups. It started in Uppsala by Siegbahn and co-workers in the 1970's where in-house based systems for gases at high pressures and liquids were developed.[16–19] These laboratory based systems were followed by installations at synchrotron radiation facilities.[19–23] Recently, high performing laboratory based HPXPS systems have again emerged, and the technique is now commercially available.[15,24,25]

When it comes to battery research, the new HPXPS instrumental developments allow for XPS measurement under more realistic battery operating conditions. In some of the HPXPS instruments, measurements at pressures of up to 25 mbar are possible.[15,26,27] Although this does not fully reach atmospheric conditions, this pressure is higher than the vapor pressure of

a)E-mail: maria.hahlin@physics.uu.se

many Li-ion battery electrolyte solvents, and, most importantly, these pressures allow liquid electrolyte to be present within the analysis chamber of a HPXPS instrument. This is a remarkable step forward in instrumentation usability when it comes to understanding batteries in operando at an element specific chemical level.

To date, only a few published articles on *in situ* HPXPS studies of Li-ion batteries can be found.[28–30] In these, it has been demonstrated that HPXPS can be used for following the electrochemical processes in batteries and obtaining new insights into the reaction mechanism in the Li-air chemistry. Common for the investigated systems is, however, that they do not contain the interface between the solid electrode and the electrolyte. In this article, we present a versatile HPXPS method for measuring directly at the solid/liquid interface that can be swiftly implemented on Li-ion battery systems. The battery is not exposed to air and needs no intermediate UHV sample introduction step. This article reports for the first time HPXPS results on the SEI layer at which also the carbonate based liquid electrolyte is present.

MATERIALS AND EXPERIMENTAL

The Si|$LiClO_4$ in propylene carbonate (PC)|Li battery system was chosen as a model system. The electrolyte solvent PC was chosen due to its low vapor pressure of 0.04 mbar at 20 °C.[31] Silicon was selected as model electrode material since it is considered to be the most promising anode material for next generation lithium ion batteries due to its high gravimetric capacity (~3600 mAh/g, almost 10 times higher than conventional graphite electrode).[32,33] However, Si anodes suffer from large volume changes during cycling (up to 400% expansion during lithiation), which results in problems such as high mechanical stress, active material loss, and loss of electric contact.[34,35] Therefore, an electrochemically and physically stable SEI is essential for these batteries to achieve long time cycling without rapid capacity fading.

Silicon electrodes were prepared by coating a slurry of silicon nano-powder (Alfa Aesar), super-P carbon black (Erachem Comilog), and sodium carboxymethyl cellulose (CMC-Na, Sigma Aldrich) with a mass ratio of 80:12:8 onto a copper foil. The slurry was first ball-milled for 1 h and then casted on the Cu foil using doctor-blading. The electrodes were punched with a diameter of 20 mm and dried under vacuum at 120 °C for 12 h. The mass loading of the electrode coating was approximately 1.7 mg per punched electrode. The electrolyte used was 1 M $LiClO_4$ (Aldrich) in PC (NOVOLYTE technologies). The salt was dissolved in PC and stirred for 3 days. The salt $LiClO_4$ was dried under vacuum at 80 °C for 12 h prior to the electrolyte preparation.

The Silicon|electrolyte|Li half-cell was assembled inside an Argon-filled glove box (O_2 < 2 ppm, H_2O < 1 ppm) by sandwiching an electrolyte-soaked Solupor polymer separator between the respective Si and Li electrodes and subsequent vacuum-sealing of the stack into a pouch cell. The battery was cycled at a current density of 250 mA/g between 0.01 V and 0.9 V (vs. Li/Li^+) for 1 cycle. All electrodes were washed and individually vacuum-sealed inside the glove box to be transported to the measurement station without air contact.

The HPXPS setup (see Figure 1) contained a Scienta R4000 HiPP-2 high pressure analyzer and a monochromatized Scienta MX650 HP AlKα X-ray source combined in a system equipped with an analysis chamber, a load lock chamber, and a manipulator, as reported in Ref. 26. The analyzer was operated using the swift acceleration mode type of operation[36] using the 0.8 mm diameter front cone. The sample was placed 0.8 mm from the first aperture resulting in an actual pressure in the vincinity of the sample of at least 95% of the measured pressure.[20] The sample was introduced via the glove bag (polyethylene glove bag, 91717.LK, VWR International AB) into the load lock in a nitrogen atmosphere (99.999% Alphgaz 1™ from Air Liquide AB). All spectra are internally referenced with respect to the C1s emission of carbon black in the pristine electrode, set to 284.5 eV.[37] The spectral intensities are normalized to the number of sweeps. Direct comparison of absolute intensities is not attempted between different samples and different measurement positions. However, in cases where sample position and instrumental settings were kept constant, intensities were compared in order to follow changes with time. The intensity (peak area) was obtained by integration of the respective curve fit. The spectra were curve fitted after Shirley background subtraction using Voigt profiles with Lorentzian contribution of 20%-30%.

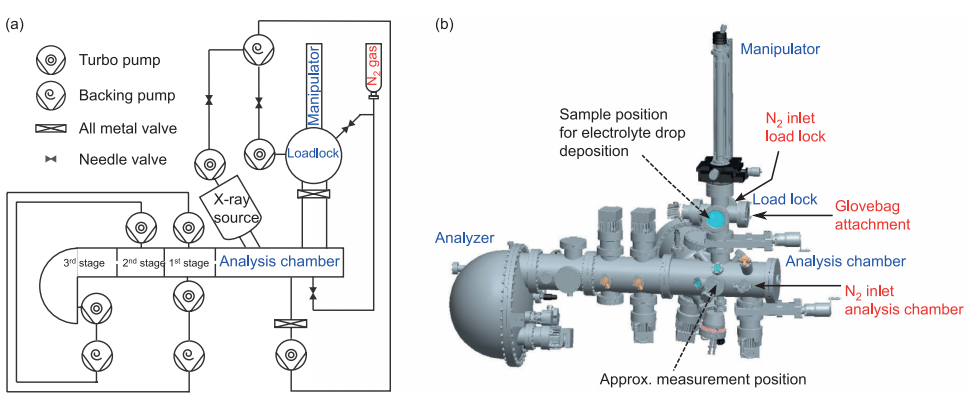

FIG. 1. Schematic representation of the HPXPS setup at VG Scienta, Uppsala. (a) Overview of the pumping and gas inlet system. (b) 3D model in which the points of attachment for the glove bag as well as the two N_2 inlets are marked by solid arrows. The dashed arrows indicate the approximate sample positions for the electrolyte drop deposition and the measurement position, respectively.

METHODOLOGY DEVELOPMENT AND EVALUATION

The development and characterization of a new sample transfer procedure aiming for HPXPS studies on solid electrode electrolyte interfaces is demonstrated. In the sections on Sample Transfer Procedure, The Electrode Electrolyte Interface, and Time Dependent Evolution of the Electrolyte Drop, the use of this transfer procedure for developing a methodology for direct measurements on wet functional interfaces is evaluated by comparing measurement positions and by following the solvent evaporation with time. Finally, the first results on an electrochemically modified battery interface are discussed in the section on The Electrode Electrolyte Interface on Electrochemically Modified Si Electrode.

Sample transfer procedure

Our previous results have shown that the sensitive nature of the battery components requires a protected environment, especially limiting exposure to H_2O and O_2, during sample handling.[38] Hence, a glove-bag was mounted on the load lock (see Figure 1(b)), which was subsequently flushed three times with N_2 gas. Inside the glove bag, a vacuum-sealed bag containing a pristine Si-electrode was opened and the electrode was positioned on the HPXPS manipulator inside the load lock. Once in place, a drop of electrolyte was deposited on the pristine electrode, followed by a fast pump down to HPXPS conditions (e.g., 2 mbar or other desired operating pressure). The instrumental construction allowed for separate control of the vacuum conditions of the load lock and the analysis chamber (i.e., two individual pumping systems and N_2 gas inlets, see Figure 1), and thus simultaneously, a 2 mbar atmosphere set by the N_2 amount was created within the chambers. Once this condition of equal N_2 pressures was established, the valve between the load lock and analysis chamber was opened, and the sample was moved to measurement position. With this procedure, the sample is never exposed to high vacuum conditions, and thus, the electrolyte is still present as a liquid drop on the electrode. To our knowledge, this is the first time samples are moved from controlled atmospheric pressure conditions directly into HPXPS conditions without passing high vacuum. Importantly, this procedure opens for HPXPS investigations of samples sensitive to vacuum, e.g., direct study of wet chemistry samples. The time elapsed between first pumping and start of the measurements was typically only 15-30 min. Figure 2 shows pictures from the sample transfer procedure; the dropping of the electrolyte on the pristine electrode inside the load lock (Figure 2(a), position within the setup indicated in Figure 1) and the sample in measurement position, where the drop of electrolyte is clearly visible (Figure 2(b), position in the setup indicated in Figure 1).

A key advantage with the method is that it does not require a high vacuum sample introduction step, and from Figure 2(b), it is clear that this sample transfer procedure yields a battery sample that can be analyzed with both solid and liquid present. This is demonstrated for a sample prepared by drop of a PC based electrolyte deposited on a Si electrode (see Figure 3) introduced to UHV and 2 mbar sample pressure, respectively. When using the new method (i.e., 2 mbar spectrum), the characteristic emissions of the electrolyte solvent PC are visible as indicated by the dotted lines.

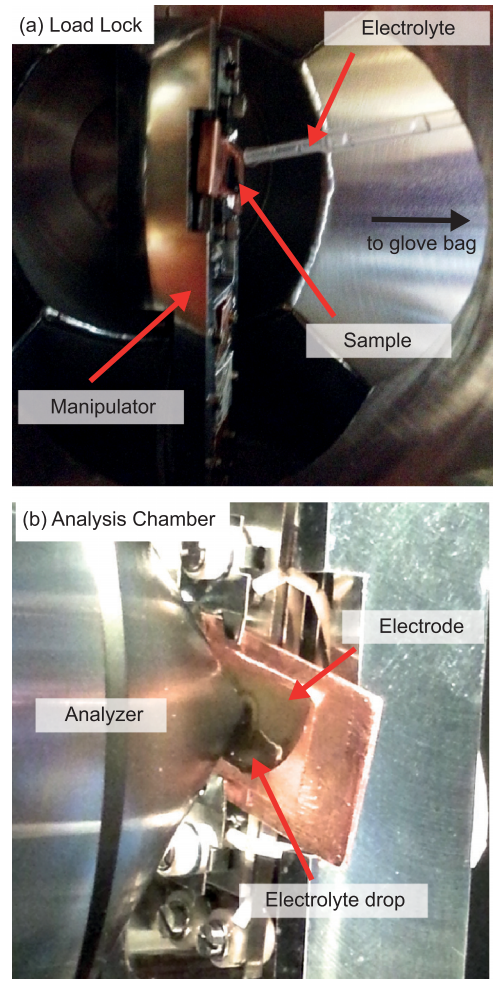

FIG. 2. The sample transfer procedure including (a) the electrode placed on the manipulator inside the load lock, and a drop of the electrolyte is deposited on its surface and (b) the sample in 2 mbar HPXPS measurement position, where the liquid electrolyte is clearly visible.

The electrode electrolyte interface

After successful transfer of the electrode with a liquid drop of electrolyte, HPXPS measurements were performed at different sample positions. When moving the sample in the vertical direction with respect to the analyzer, we observed that the differential pumping through the analyzer front cone affects the position of the liquid drop (as can be seen in Figure 2(b)). The results clearly confirm the presence of the liquid state of the electrolyte, which, as demonstrated below, can be used to access the electrode electrolyte interface.

The corresponding Si2p, C1s (with the Cl2s on the lower binding energy side), and O1s spectra for the respective positions are represented in Figures 4(a)-4(c), where the bottom spectra correlate to the measurement position directly at the drop of electrolyte, the middle spectra were recorded for the intermediate measurement position, and the top spectra correspond to a dry Si-electrode as reference, as indicated in Figure 4(d).

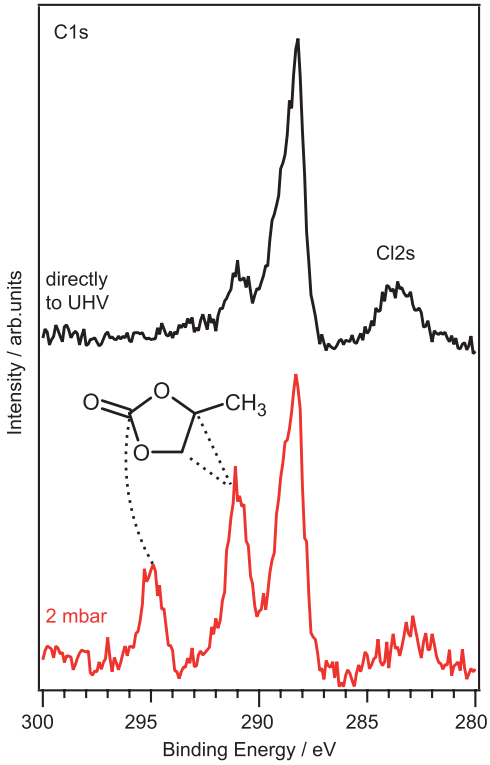

FIG. 3. Comparison of C1s spectra of a drop of electrolyte on a Si electrode introduced to UHV (black) and 2 mbar (red) sample pressure, respectively. The characteristics of the electrolyte solvent PC are indicated by the dotted lines.

From the evolution of Si2p, C1s, and O1s photoemissions, it is clear that the different sample positions give different relative core level intensities in a comparison between peaks originating from the solid and liquid. In the Si2p region for the interface measurement position and the reference electrode, all observed emission lines are attributed to the bulk solid electrode. No distinct Si2p emission could be observed for the measurement at the regions of the sample with a visually observable electrolyte drop. This indicates that the thickness of the drop is well beyond three times the inelastic mean free path of the photoelectrons generated at the solid electrode electrolyte interface at the corresponding kinetic energy.[39] Consequently, the obtained carbon and oxygen emissions are predominantly attributed to the electrolyte for this sample position. The presence of the electrolyte is also confirmed by the Cl2s signal at around 280 eV originating from the salt $LiClO_4$ (Cl2p binding energy given in Ref. 40, binding energy difference between Cl2p and Cl2s taken from Ref. 37).

In the C1s spectrum of the liquid electrolyte, the two higher binding energy peaks are attributed to the carbon atom in the carbonate and ester position in the PC molecule based on their characteristic binding energy difference.[41] These distinct contributions from the solvent PC are indicated by the dotted lines in Figure 4. The most intense C1s line most likely originates from the methyl group as well as adsorbed hydrocarbons indicating that the transfer system relying on a glove bag is not ideal in terms of prevention of contaminations. Additionally, it cannot be excluded that carbon containing species from the electrode have dissolved in the liquid electrolyte and accumulate at the droplet surface. Contribution from the solid electrode material in the position referred to as electrolyte may be fully excluded as the photoelectrons at the C1s (and O1s) core level have lower kinetic energy than the electrons stemming from Si2p and the latter is not observed.

To unequivocally access information from the interface, the sample is moved in a vertical direction in front of the analyzer. For the interface measurement position, a clear Si2p signal is obtained corresponding to the Si2p signal of the

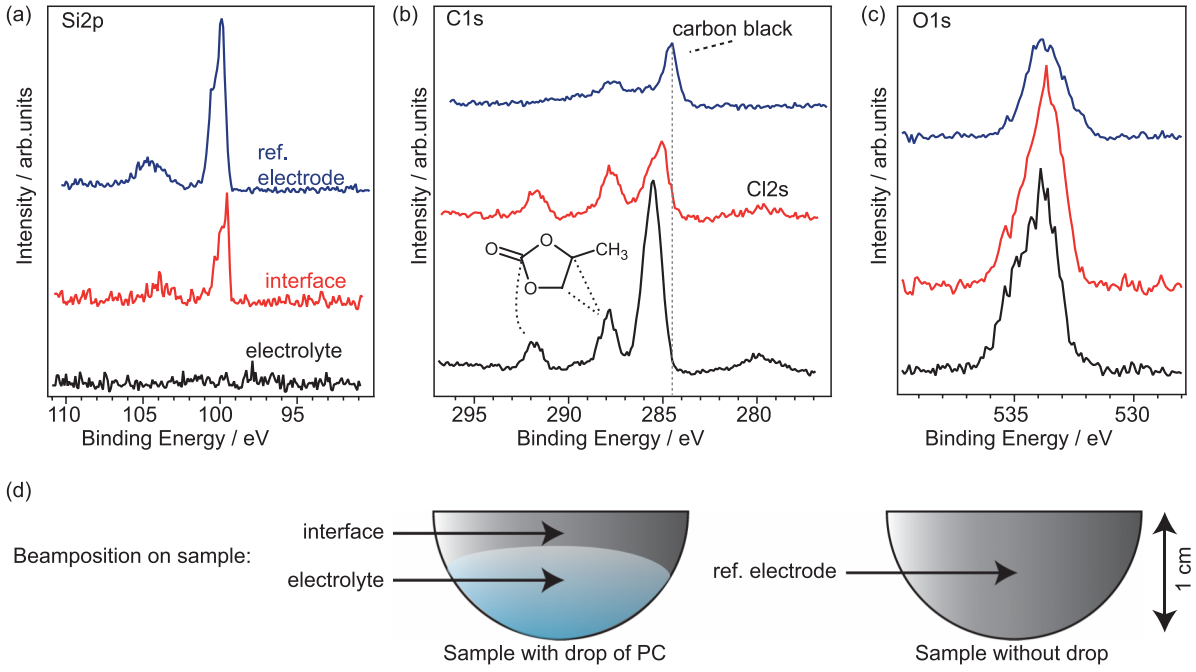

FIG. 4. The core level spectra (Si2p, C1s/Cl2s, and O1s) corresponding to different samples/sample positions are shown in (a)-(c) respectively, in which the reference electrode has blue, the interface red, and electrolyte black color code. Approximate beam positions for the individual measurements are indicated in the schematic picture (d).

pristine electrode. In the carbon and oxygen emissions, the peaks expected for the PC based electrolyte are observed. Additionally, changes in line-shape compared to the electrolyte spectra can be observed also indicating substrate and potentially specific interfacial contributions. This becomes evident (i) in the C1s spectra in the changed intensity ratio between the carbonate ester component at 292 eV and the main carbon emission at 286 eV, which is also broadened due to the overlap with the substrate carbon black peak and (ii) in the O1s spectra in the intensity increase of the low binding energy oxygen component assigned to bulk electrode (SiO_x and CMC binder) with respect to the shoulder at higher binding energies (i.e., 536 eV). Moreover, the O1s emission in the interface spectrum can be described as a superposition of electrode and PC signal by taking the reduction in Si2p intensity between the reference electrode and interface spectra as a measure for the damping of the substrate signal. The presence of both substrate and electrolyte emissions shows that the interface region between solid and liquid is probed.

The presented results clearly demonstrate that with this approach, it is possible to obtain information about the functional solid-liquid interface between electrode and electrolyte using HPXPS.

Time dependent evolution of the electrolyte drop

To study the behavior of the liquid electrolyte during HPXPS measurements in more detail, time dependent studies at different sample pressures have been performed. The sample pressures were set by the N_2 amount. The core level spectra were recorded for a drop of electrolyte on an electrode at 2 mbar as a function of time. These measurements were followed by measurements at UHV conditions. Similar measurements for a drop of electrolyte on an electrode at 0.7 mbar pressure with following pressure reduction to 0.3 mbar and subsequently to UHV conditions were performed. In Figure 5 the time evolution of the O1s and C1s spectra at 2 mbar and subsequently UHV is shown. The zero point of the time scale refers to the starting time of the pumping process (from N_2 atmospheric pressure to the mbar region) during sample introduction.

Both the O1s and the C1s emissions undergo a continuous change in line shape with increasing time between the first and last measurements at 2 mbar. Once under UHV conditions, the spectral characteristics have changed drastically. Specifically, in the C1s spectrum, the intensity of the two higher binding energy components at 292.2 eV and 288 eV originating from PC decreases with time relative to the C1s component at 286 eV. At UHV conditions, the two higher binding energy PC components have vanished. Additionally, the emissions at 288 eV and 286 eV shift towards lower binding energies. In the O1s spectrum, the line shape gradually changes from two clearly resolved peaks with one at 535.4 eV and a second at around 533.5 eV to a single, broad peak positioned at 534 eV at UHV conditions. Additionally, an increase in the Si2p emission from the substrate was detectable from 93 min on (see supplementary figure S1[42]). The same qualitative change in line shapes could be observed for the measurements at 0.7 mbar with subsequent pressure adjustment to 0.3 mbar

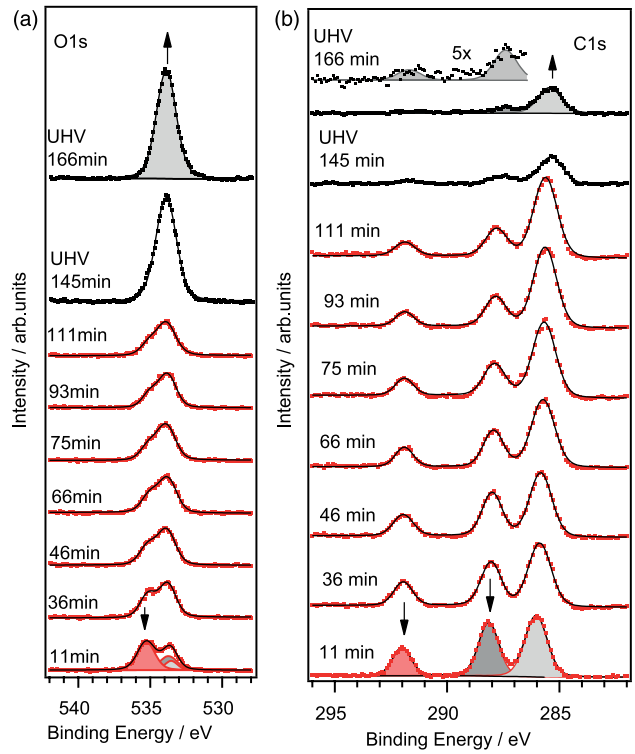

FIG. 5. Evolution of the O1s (a) and C1s (b) core level at 2 mbar and subsequent UHV exposure as a function of time for a drop of electrolyte on as Si electrode. The original data are represented as dotted lines (red 2 mbar and black UHV), while the overall fitting results are represented as solid black lines. The areas used for the following intensity analysis are shaded in red, while the other fitted emissions in the C1s and O1s stemming from PC and the electrode are shaded gray. The black arrows pointing downwards indicate decreasing PC components (at 535.4 eV in O1s and 292.2 eV as well as 288 eV in C1s). The arrows pointing up in the top UHV spectra indicate the increasing electrode substrate emissions (at 534 eV in O1s and 285 eV in C1s).

after 80 min and followed by UHV measurements, only the changes are much more pronounced also for shorter times in case of lower pressures (see supplementary figure S2[42]). Qualitatively, all these observations are in line with solvent evaporation leading to a reduced droplet thickness and thus increased substrate signal intensity. We therefore conclude that the thickness of the liquid electrolyte layer during the procedure is within range of the XPS information depth allowing us to probe both the electrolyte as well as the electrode.

In order to further quantify the spectral changes with time and pressure, the PC contributions in the C1s and O1s spectra were determined. The overall curve fitting results are represented by solid lines while the original data points are given as dotted lines in Figure 5. To exemplify the de-convolution, the separate components are shown as shaded areas for the spectra obtained at 11 min and 166 min in Figure 5. The C1s carbonate ester component (shaded red) is not overlapping with any other component and is thus chosen for primary evaluation of the electrolyte intensity with time. Due to overlapping oxygen emissions from substrate and electrolyte, the intensity evaluation of the O1 is more complex; however, in combination with the C1s carbonate ester evaluation, it can provide information about the solvent. Therefore, also the oxygen emission at 535.4 eV originating from the ether oxygen atoms in PC is chosen for evaluation. The obtained

peak areas from the respective curve fits are plotted as intensities relative to the initial intensity (i.e., relative to the first recorded spectrum taken at 11 min) versus the time elapsed between measurements and first pumping in Figure 6(a). It is clear that the relative intensity of both the evaluated C1s and O1s components initially decrease rather steadily. The rate of intensity decrease is very similar in carbon and oxygen indicating that the whole PC molecules evaporate.

Plotted in Figure 6(b) is the relative intensity of the carbonate ester component for the measurements starting at 2 mbar and 0.7 mbar, respectively. For a starting pressure of 0.7 mbar, the decrease in relative intensity is faster compared to the measurements starting at 2 mbar, as can be seen from the steeper slope described by the individual green squares compared to the red diamonds in Figure 6(b). These results are interpreted as that the N_2 base pressure influences the rate of PC evaporation, where a higher base pressure decreases the rate of evaporation. As the vapor pressure itself is almost independent on the ambient pressure in the analysis chamber,[43] this can be explained by diffusion limitation with increased pressure: The diffusion of the evaporating PC molecules through the analyzer front cone will be slowed down by the addition of N_2 molecules. This reduces the pumping speed of the solvent molecules and thus increases the time window in which liquid electrolyte is present.

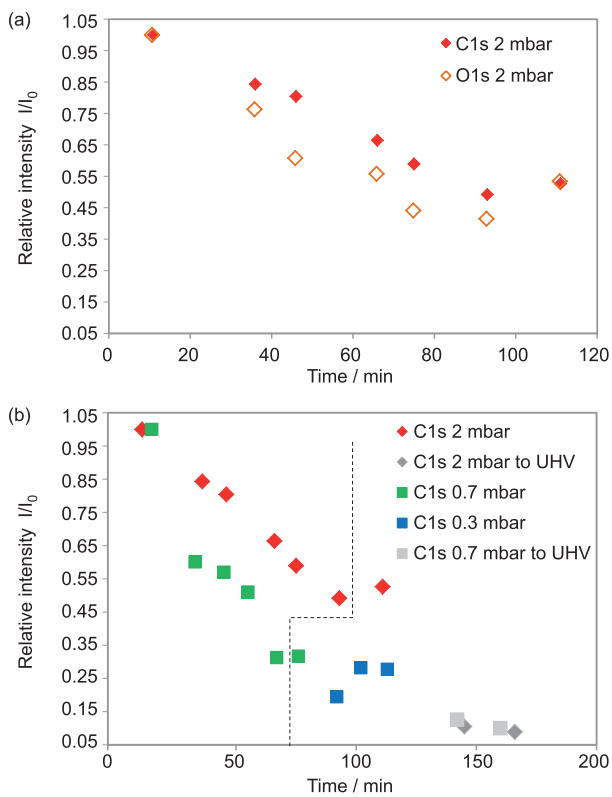

FIG. 6. Evolution of the relative intensities of the PC photoemission signals as a function of measurement pressure versus time elapsed after sample introduction. (a) C1s (solid red diamond) and O1s (open orange diamond) relative intensity changes for 2 mbar starting pressure. (b) C1s relative intensity change for 2 mbar (solid red diamonds), 0.7 mbar (solid green squares) with a subsequent 0.3 mbar (solid blue squares), at UHV conditions after both the 2 mbar (solid grey diamonds), and the 0.3 mbar (solid grey squares) measurements. The dotted line indicates the time frame for liquid electrolyte measurements.

After a pumping step of 30 min going from 2 mbar and 0.3 mbar, respectively, to UHV, the relative intensities of the carbonate ester C1s component is reduced to below 0.1 for both samples. The sample measured at 2 mbar was kept in UHV for additional 66 h. In the spectra recorded after this time-period, no emissions from PC could be detected (not shown) indicating complete desorption of PC as also observed when going to UHV directly (see Figure 3).

The rate of solvent evaporation appears to slow down to a minimum after a certain measurement time, seen as the flattening and convergence of the data points at around half the original intensity for 2 mbar and around 1/3 of the original intensity for the 0.7 mbar measurements (Figure 6(b)). For the 2 mbar measurement, this occurs after around 90 min, while for the 0.7 mbar measurement, this occurs after around 70 min. The convergence in evaporation rate is particularly evident when observing the almost unchanged relative C1s intensity when decreasing the pressure from 0.7 mbar to 0.3 mbar (blue squares in Figure 6(b)). Combined, these results indicate a change in the liquid electrolyte structure that affects the rate of evaporation. It can be speculated that this may be linked to an increased electrolyte salt concentration in the remaining liquid. At the time when the rate flattening is observed, intermolecular interactions could become stronger and thus reduce the rate of solvent evaporation. For the HPXPS methodology presented here, this implies that although the time frame of investigating the original electrolyte composition is limited, there is a time frame for measuring a wet surface. Moreover, combining this with the possibility to vary the sample position, it is clear that the important interactions at the solid electrode electrolyte interface can be probed. Specifically from this article, it is estimated that using 2 mbar N_2 sample pressure for the 1 M $LiClO_4$ in PC electrolyte yields a measurement time frame for studying the solid electrode electrolyte interface of approximately 90 min.

The electrode electrolyte interface on electrochemically modified Si electrode

The developed methodology may be used to study applications where the key function lies in the interactions between a solid sample and a liquid electrolyte. This method was therefore used for the investigation of an electrochemically cycled silicon electrode. Prior to the HPXPS measurements, the silicon electrode was cycled versus lithium using an electrolyte consisting of 1 M $LiClO_4$ in PC, thus forming the SEI on the electrode surface. The electrochemical performance is provided in Figure S3.[42] The goal of these HPXPS measurements is to investigate the SEI properties in presence of the liquid electrolyte. The preliminary characterization was carried out on fully delithiated silicon electrodes taken directly from cycled batteries. The measurements were performed at different time intervals at 2 mbar N_2 pressure and subsequent at UHV (ca. 30 min pumping from 2 mbar to UHV). The XPS results are shown in Figure 7. The characteristic emissions of PC showed its evaporation also in this case (C1s peak at 292 eV and O1s peaks at 535.4 eV). As time evolves, the intensities of these characteristic solvent peaks decrease and are no longer visible for the subsequent UHV measurement.

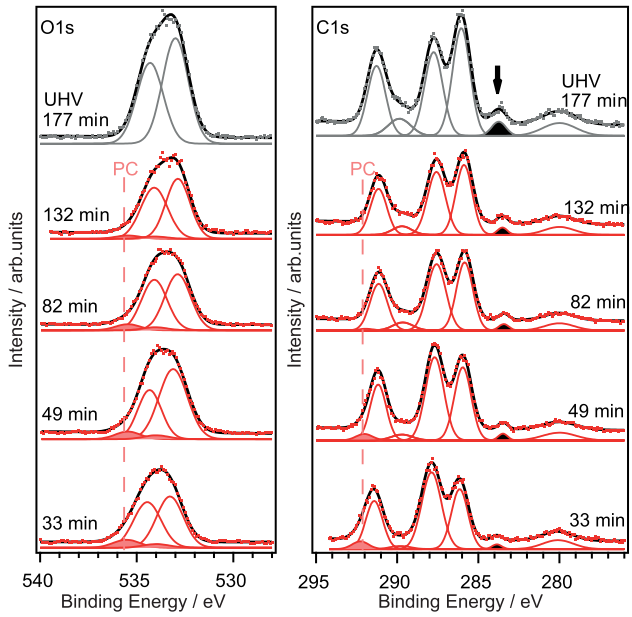

FIG. 7. Evolution of C1s and O1s spectra at 2 mbar (red) and subsequent UHV (grey) for a fully delithiated silicon electrode as a function of time. The electrodes were cycled with 1 M $LiClO_4$ in PC electrolyte. The carbon black spectral contribution is highlighted in black.

The carbon black peak (black in Figure 7) at ca. 283.5 eV becomes more pronounced as the PC emissions decrease. Since the carbon black only exists in the solid substrate electrode, the observation of its signal is a clear sign that the HPXPS measurement can probe the bulk through the complete SEI layer. The relative peak structures originating from the SEI are rather stable with time, and the main difference is primarily due to the evaporation of the solvent. The SEI layer in this study mainly consists of Li_2CO_3 (C1s at 291.3 eV are O1s at 533 eV), polyether-like compounds, (O1s at 534.2 eV and C1s at 288 eV) and hydrocarbon species beside the $LiClO_4$ salt residue from the electrolyte. Thus, the here measured SEI composition is similar to that observed in previous XPS studies on carbonaceous electrodes that have been cycled with PC-based liquid electrolytes and where the formed SEI layer is dominated by polyether-, hydrocarbon-, and carbonate-species.[3,44] These first HPXPS results show that the SEI formed on the Si-anode under present conditions is largely unaffected by the liquid solvent, and that UHV based studies on dry samples give a reasonable representation of the composition of the SEI in a complete device.

These results imply that the real benefit from HPXPS studies of battery samples comes when going to operando measurements. Many of the components suggested to form within the SEI are highly reactive and may react further with the surrounding components, in this way forming the SEI.[3] With operando HPXPS, these initial chemical reactions can be followed. The open design of the HPXPS introduction and analysis chamber used in this study,[26] allowing insertion of samples without exposure to high vacuum, yields the possibility to maintain a liquid electrolyte during HPXPS measurements. This in turn allows for a simple full battery sample design for operando HPXPS measurements by including electrical feedthroughs and a counter electrode at the position of the probed electrode. For operando battery system analysis, improvements to the measurements should include, e.g., better sample transfer equipment or integration of a glovebox with the HPXPS instrument to further reduce air exposure.[38] Replacing the N_2 gas with Ar would also eliminate the possibility of Li_3N formation in cases where metallic Li is present in the sample.[45] Moreover, a more stable electrolyte composition can be achieved by saturating the atmosphere in the analysis chamber with solvent molecules, e.g., by introducing electrolyte solvent at its vapor pressure into the analysis compartment. In realizing this, the chemical processes building up the SEI can be followed in real time yielding increased understanding of the SEI formation process, ultimately leading to improved battery performance.

CONCLUSIONS

For the first time, we present high pressure photoelectron spectroscopy results of the solid/liquid interface in Li-ion batteries based on a silicon negative electrode and a PC/$LiClO_4$ electrolyte as a model system. The presence of liquid electrolyte at the electrode surface was achieved by designing a sample preparation and transfer procedure that allowed the introduction of electrochemical samples into the analysis chamber without an intermediate UHV step. The liquid drop was maintained for a sufficiently long period to perform the HPXPS characterizations by introducing a base pressure of N_2 in the range of a few millibars, which leads to a significantly shorter mean free path of the evaporating solvent molecules compared to the mean free path of the emitted photoelectrons.

By moving the sample in the vertical direction with respect to the analyzer inlet cone, the region showing the full solid/electrolyte interface was pinpointed. It is demonstrated that for the given system, the solid electrode electrolyte interface can be considered stable for time well within the time frame to conduct thorough HPXPS analysis.

Results obtained from the electrochemically modified Si electrode with liquid electrolyte showed the presence of an SEI with a similar composition as observed in measurements at UHV sample pressures. This proves the relevance of previously published UHV XPS studies of the formed SEI and moreover underlines that the investigated solid electrode electrolyte interfaces, obtained via the high pressure sample transfer technique described here, are stable.

It is expected that a combination of our transfer technique with *in situ*/operando studies using both hard x-ray photoelectron spectroscopy and high pressure (HP-HAXPES) will yield deeper insights to important intermediate electrochemical processes. Specifically, compositional changes in the liquid electrolyte, solid electrode, and at their interface could be investigated simultaneously.

ACKNOWLEDGMENTS

The research leading to these results has received funding from the European Union's Seventh Framework Programme (FP7/2007-2013) under Grant Agreement No. 608575. Additionally, we gratefully acknowledge StandUp for Energy,

Swedish Energy Agency and the Swedish Research Council (Grant No. 2012-4681) for financial support. VG Scienta acknowledges funding from Swedish Governmental Agency for Innovation Systems (VINNOVA) for the development of the Scienta HiPP-2 instrument.

[1]J. M. Tarascon and M. Armand, "Issues and challenges facing rechargeable lithium batteries," Nature **414**(6861), 359-367 (2001).
[2]E. Peled, "The electrochemical behavior of alkali and alkaline earth metals in nonaqueous battery systems—The solid electrolyte interphase model," J. Electrochem. Soc. **126**(12), 2047-2051 (1979).
[3]K. Xu., "Nonaqueous liquid electrolytes for lithium-based rechargeable batteries," Chem. Rev. **104**(10), 4303-4418 (2004).
[4]D. Aurbach *et al.*, "Identification of surface films formed on lithium in propylene carbonate solutions," J. Electrochem. Soc. **134**(7), 1611-1620 (1987).
[5]P. Verma, P. Maire, and P. Novak, "A review of the features and analyses of the solid electrolyte interphase in Li-ion batteries," Electrochim. Acta **55**(22), 6332-6341 (2010).
[6]K. C. Högström *et al.*, "The influence of PMS-additive on the electrode/electrolyte interfaces in LiFePO4/graphite Li-ion batteries," J. Phys. Chem. C **117**(45), 23476-23486 (2013).
[7]M. Y. Nie *et al.*, "Silicon solid electrolyte interphase (SEI) of lithium ion battery characterized by microscopy and spectroscopy," J. Phys. Chem. C **117**(26), 13403-13412 (2013).
[8]C. Xu. *et al.*, "Interface layer formation in solid polymer electrolyte lithium batteries: An XPS study," J. Mater. Chem. A **2**(20), 7256-7264 (2014).
[9]L. Yang, B. Ravdel, and B. L. Lucht, "Electrolyte reactions with the surface of high voltage LiNi0.5Mn1.5O4 cathodes for lithium-ion batteries," Electrochem. Solid State Lett. **13**(8), A95-A97 (2010).
[10]B. Philippe *et al.*, "Nanosilicon electrodes for lithium-ion batteries: Interfacial mechanisms studied by hard and soft X-ray photoelectron spectroscopy," Chem. Mater. **24**(6), 1107-1115 (2012).
[11]V. Etacheri *et al.*, "Effect of fluoroethylene carbonate (FEC) on the performance and surface chemistry of Si-nanowire Li-ion battery anodes," Langmuir **28**(1), 965-976 (2012).
[12]B. Philippe *et al.*, "Role of the LiPF6 salt for the long-term stability of silicon electrodes in Li-ion batteries–A photoelectron spectroscopy study," Chem. Mater. **25**(3), 394-404 (2013).
[13]S. Malmgren *et al.*, "Comparing anode and cathode electrode/electrolyte interface composition and morphology using soft and hard X-ray photoelectron spectroscopy," Electrochim. Acta **97**, 23-32 (2013).
[14]K. C. Högström *et al.*, "Aging of electrode/electrolyte interfaces in LiFePO4/graphite cells cycled with and without PMS additive," J. Phys. Chem. C **118**(24), 12649-12660 (2014).
[15]D. E. Starr *et al.*, "Investigation of solid/vapor interfaces using ambient pressure X-ray photoelectron spectroscopy," Chem. Soc. Rev. **42**(13), 5833-5857 (2013).
[16]K. Siegbahn, "From X-Ray to electron-spectroscopy and new trends," J. Electron Spectrosc. Relat. Phenom. **51**, 11-36 (1990).
[17]M. Faubel, B. Steiner, and J. P. Toennies, "Photoelectron spectroscopy of liquid water, some alcohols, and pure nonane in free micro jets," J. Chem. Phys. **106**(22), 9013-9031 (1997).
[18]B. Winter and M. Faubel, "Photoemission from liquid aqueous solutions," Chem. Rev. **106**(4), 1176-1211 (2006).
[19]M. A. Brown *et al.*, "A new endstation at the Swiss Light Source for ultraviolet photoelectron spectroscopy, X-ray photoelectron spectroscopy, and X-ray absorption spectroscopy measurements of liquid solutions," Rev. Sci. Instrum. **84**(7), 073904 (2013).
[20]D. F. Ogletree *et al.*, "Photoelectron spectroscopy under ambient pressure and temperature conditions," Nucl. Instrum. Methods Phys. Res., Sect. A **601**(1–2), 151-160 (2009).
[21]J. Schnadt *et al.*, "The new ambient-pressure X-ray photoelectron spectroscopy instrument at MAX-lab," J. Synchrotron Radiat. **19**(5), 701-704 (2012).
[22]M. E. Grass *et al.*, "New ambient pressure photoemission endstation at advanced light source beamline 9.3.2," Rev. Sci. Instrum. **81**(5), 053106 (2010).
[23]H. Bluhm, "Photoelectron spectroscopy of surfaces under humid conditions," J. Electron Spectrosc. Relat. Phenom. **177**(2–3), 71-84 (2010).
[24]F. Mangolini *et al.*, "Angle-resolved environmental X-ray photoelectron spectroscopy: A new laboratory setup for photoemission studies at pressures up to 0.4 Torr," Rev. Sci. Instrum. **83**(9), 093112 (2012).
[25]F. Tao, "Design of an in-house ambient pressure AP-XPS using a bench-top X-ray source and the surface chemistry of ceria under reaction conditions," Chem. Commun. **48**(32), 3812-3814 (2012).
[26]S. K. Eriksson *et al.*, "A versatile photoelectron spectrometer for pressures up to 30 mbar," Rev. Sci. Instrum. **85**(7), 075119 (2014).
[27]S. Kaya *et al.*, "Ambient-pressure photoelectron spectroscopy for heterogeneous catalysis and electrochemistry," Catal. Today **205**, 101-105 (2013).
[28]Y.-C. Lu. *et al.*, "*In situ* ambient pressure X-ray photoelectron spectroscopy studies of lithium-oxygen redox reactions," Sci. Rep. **2**, 715 (2012).
[29]E. J. Crumlin, H. Bluhm, and Z. Liu, "*In situ* investigation of electrochemical devices using ambient pressure photoelectron spectroscopy," J. Electron Spectrosc. Relat. Phenom. **190**, 84-92 (2013).
[30]Y.-C. Lu. *et al.*, "Influence of hydrocarbon and CO2 on the reversibility of Li–O2 chemistry using *in situ* ambient pressure X-ray photoelectron spectroscopy," J. Phys. Chem. C **117**(49), 25948-25954 (2013).
[31]Sigma-Aldrich®, 2014-08-20, Available: http://www.sigmaaldrich.com/catalog/product/sial/310328?lang=en&region=SE.
[32]V. Etacheri *et al.*, "Challenges in the development of advanced Li-ion batteries: A review," Energy Environ. Sci. **4**(9), 3243-3262 (2011).
[33]M. N. Obrovac and L. Christensen, "Structural changes in silicon anodes during lithium insertion/extraction," Electrochem. Solid State Lett. **7**(5), A93-A96 (2004).
[34]R. Benedek and M. M. Thackeray, "Lithium reactions with intermetallic-compound electrodes," J. Power Sources **110**(2), 406-411 (2002).
[35]M. J. Chon *et al.*, "Real-time measurement of stress and damage evolution during initial lithiation of crystalline silicon," Phys. Rev. Lett. **107**(4), 045503 (2011).
[36]M. O. M. Edwards *et al.*, "Increased photoelectron transmission in High-pressure photoelectron spectrometers using 'swift acceleration,"' Nucl. Instrum. Meth. A **785**, 191 (2015).
[37]J. F. Moulder *et al.*, *Handbook of X-Ray Photoelectron Spectroscopy* (Physical Electronics, Inc., 1995).
[38]S. Malmgren *et al.*, "Consequences of air exposure on the lithiated graphite SEI," Electrochim. Acta **105**, 83-91 (2013).
[39]S. Hüfner, *Photoelectron Spectroscopy: Principles and Applications*, 3rd ed. (Springer, Berlin, Heidelberg, New York, 2003).
[40]D. Martin-Vosshage and B. V. R. Chowdari, "XPS studies on (PEO) n LiClO4 and (PEO) n Cu(ClO4)2 polymer electrolytes," J. Electrochem. Soc. **142**(5), 1442-1446 (1995).
[41]G. Beamson and D. Briggs, *High Resolution XPS of Organic Polymers: The Scienta ESCA300 Database* (John Wiley & Sons, Ltd., West Sussex, England, 1992).
[42]See supplementary material at http://dx.doi.org/10.1063/1.4916209 for additional data on the time dependent evolution of the Si2p peak, the C1s and O1s spectral data of measurements at lower pressures (0.7 and 0.3 mbar), and the electrochemical performance data of the Si electrode cycled versus Li metal.
[43]P. Atkins and J. De Paula, *Physical Chemistry*, 7th ed. (Oxford University Press, 2002).
[44]K. Xu. *et al.*, "Chemical analysis of graphite/electrolyte interface formed in LiBOB-based electrolytes," Electrochem. Solid State Lett. **6**(7), A144-A148 (2003).
[45]D. J. David *et al.*, "Surface reactions of lithium with the environment," Appl. Surf. Sci. **7**(3), 185-195 (1981).